Short Note

A New Trigger Criterion for Improved Real-Time Performance of Onsite Earthquake Early Warning in Southern California

by M. Böse, E. Hauksson, K. Solanki, H. Kanamori, Y.-M. Wu, and T. H. Heaton

Abstract   We have implemented and tested an algorithm for onsite earthquake early warning (EEW) in California using the infrastructure of the Southern California Seismic Network (SCSN). The algorithm relies on two parameters derived from the initial 3 sec of P waveform data at a single seismic sensor: period parameter τ_c and high-pass filtered displacement amplitude P_d. Previous studies have determined empirical relationships between τ_c and the moment magnitude M_w of an earthquake, and between P_d and the peak ground velocity (PGV) at the site of observation. In 2007, seven local earthquakes in southern California with $4.0 \le M_L \le 4.7$ have triggered the calculation of M_w and PGV by the EEW algorithm. While the mean values of estimated parameters were in the expected range, the scatter was large, in particular for the smallest events. During the same time period the EEW algorithm produced a large number of false triggers due to low trigger thresholds. To improve the real-time performance of the onsite approach, we have developed a new trigger criterion that is based on combinations of observed τ_c and P_d values. This new criterion removes 97% of previous false triggers and leads to a significant reduction of the scatter in magnitude estimates for small earthquakes.

Introduction

Earthquake early warning (EEW) systems make use of differences between the propagation speed of seismic and electromagnetic waves and issue warnings, if necessary, to potential users before strong shaking at the user sites occurs. The maximal warning time of an EEW system is generally defined as the time span between the P-wave detection at the first triggered EEW sensor and the arrival of high-amplitude S or surface waves at the user site. As these time periods usually are extremely short, EEW systems must recognize the severity of expected ground motions within a few seconds. Based on this information, suitable actions for the damage reduction can be triggered and executed (Harben, 1991; Goltz, 2002).

EEW systems face two major challenges: (1) they have to be highly reliable, which means that both missed and false alerts need to be avoided; (2) the warning times should be as large as possible. About six EEW systems are presently in operation or in testing: in Japan (Nakamura, 1988; Kamigaichi, 2004; Horiuchi *et al.*, 2005; Tsukada *et al.*, 2007), in Taiwan (Wu and Teng, 2002; Wu and Kanamori 2005a,b), in California (Allen and Kanamori, 2003; Kanamori, 2005; Allen, 2007; Cua and Heaton, 2007; Wu *et al.*, 2007; Wurman *et al.*, 2007), in Mexico (Espinosa-Aranda *et al.*, 1995), in Romania (Wenzel *et al.*, 1999; Böse *et al.*, 2007), and in

Turkey (Erdik *et al.*, 2003; Böse *et al.*, 2008). Many of these systems are operated for research purposes and do not trigger any actions so far.

EEW systems are either designed for (1) regional or for (2) onsite warning. Regional warning systems that are based on networks of seismic stations usually yield stable but late estimates of seismic source parameters and therewith warnings. Onsite warning systems, in contrast, are based on single sensor observations and allow for fast but usually less reliable estimates (Kanamori, 2005).

The California Integrated Seismic Network (CISN) has developed an infrastructure that allows for testing EEW algorithms in a real-time environment, with the objective to (1) evaluate their performance in the rapid assessment of earthquakes, as well as to (2) examine the steps required to develop a pilot EEW system in California (Hauksson *et al.*, 2006). The CISN infrastructure consists of both hardware and software systems. The latter has been jointly developed by the California Institute of Technology (Caltech), the U.S. Geological Survey (USGS), and University of California, Berkeley, building on the existing software systems by the CISN and the Advanced National Seismic System (ANSS).

Three EEW algorithms are currently tested within the CISN: ElarmS (Allen and Kanamori, 2003; Allen, 2007;

Wurman *et al.*, 2007), the Virtual Seismologist (Cua and Heaton, 2007), and the τ_c–P_d algorithm (Kanamori, 2005; Wu *et al.*, 2007). The two first algorithms are regional (network based) warning approaches, while the τ_c–P_d algorithm belongs to the group of onsite (single sensor based) warning methods (Kanamori, 2005).

In this study, we focus on the real-time performance of the τ_c–P_d algorithm in southern California. About 130 broadband stations (100 samples per second velocity data) of the Southern California Seismic Network (SCSN) as part of the CISN are presently used for the EEW testing (Fig. 1). All of the data are transmitted via digital communications (Hauksson *et al.*, 2001). Between 1 January 2007 and 31 December 2007, about 80 local earthquakes in southern California with $M_L \geq 3.0$ were reported, including the nine largest earthquakes with $4.0 \leq M_L \leq 4.7$ (see the Data and Resources section). Of course, small- and moderate-sized earthquakes with $M < 6.0$ will usually not cause damage and, therefore, do not require early warnings. However, it

is necessary to use the more frequent small events for testing and calibration of EEW algorithms and systems, because large earthquakes occur rarely.

The difficulty in using small- and moderate-sized earthquakes for testing the single station-based warning algorithms is caused by the usually low signal-to-noise (S/N) ratios of the seismograms, especially in the early P phase. To use these small earthquakes for testing, we need to set the trigger thresholds at the stations at a low level. As a consequence, however, we run the risk of a large number of false triggers produced by noise and teleseismic earthquakes. In this article, we describe a trigger criterion suitable for onsite warning that automatically recognizes and removes the majority of false triggers and that helps to stabilize the magnitude estimates for small- and moderate-sized earthquakes. Although this problem is not serious for large earthquakes, a better triggering algorithm developed for small to moderate earthquakes will be useful for improving the overall performance of EEW for large earthquakes, too.
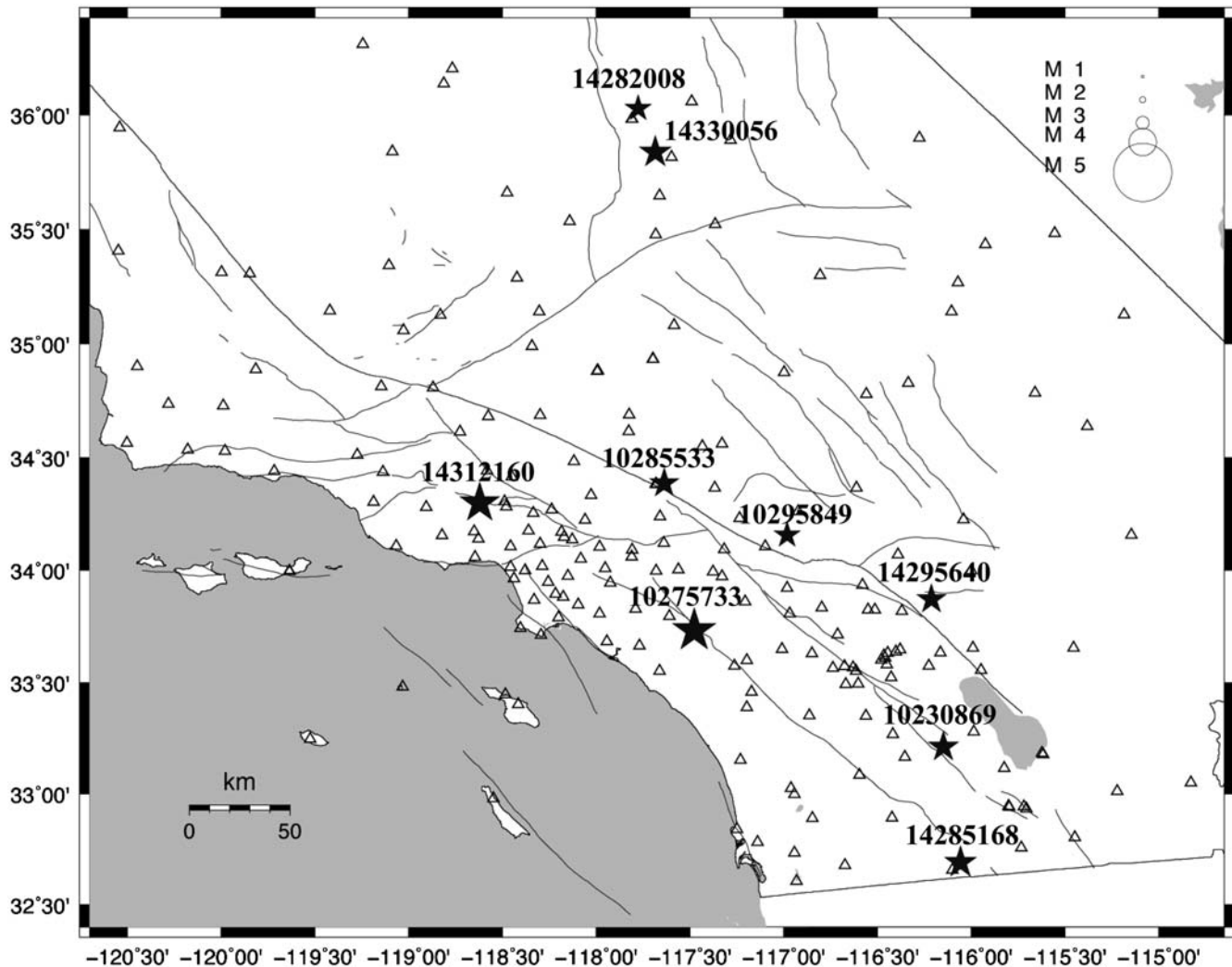

Figure 1. Distribution of broadband sensors of the Caltech/USGS SCSN used for EEW testing in southern California (triangles). Stars mark the epicentres of nine local earthquakes ($4.0 \leq M_L \leq 4.7$) analyzed in this study. Details are given in Table 1.

The τ_c–P_d Algorithm

One of the major elements of EEW is the rapid and reliable determination of earthquake magnitudes. To determine the size of an earthquake, it is important to find out whether the earthquake rupture has stopped or keeps growing. This is generally reflected in the period of the initial ground motion. Kanamori (2005) extended the method of Nakamura (1988) and Allen and Kanamori (2003) to determine a period parameter τ_c from the initial few seconds of P waves. τ_c is defined as $\tau_c = 2\pi/\sqrt{r}$ where $r = [\int_0^{\tau_0} \dot{u}^2(t)\, dt]/[\int_0^{\tau_0} u^2(t)\, dt]$, $u(t)$ is the ground-motion displacement, and τ_0 is the duration of the record used. In a series of studies (Wu and Kanamori, 2005a,b; Wu *et al.*, 2006, 2007; Wu and Kanamori, 2008a,b) τ_0 is set at 3 sec. Wu *et al.* (2007) systematically studied the records from earthquakes in southern California to explore the usefulness of τ_c for EEW purposes. They found that the moment magnitude M_{est} of an earthquake can be estimated from

$$M_{\text{est}} = 4.218 \log_{10}(\tau_c) + 6.166 \pm \sigma_{M_{\text{est}}}, \qquad (1)$$

with the standard deviation $\sigma_{M_{\text{est}}} = 0.385$.

Another important element in EEW is the estimation of the strength of S-wave shaking. Wu and Kanamori (2005b) showed that the maximum amplitude of the high-pass filtered vertical displacement during the initial 3 sec of the P wave, P_d, can be used to estimate the peak ground velocity (PGV) at the same site. Based on 780 earthquake records from Japan, Taiwan, and southern California at epicentral distances of less than 30 km, Wu and Kanamori (2008a) established an empirical relationship for estimating peak ground velocity PGV_{est} from P_d with the equation

$$\log_{10}(\text{PGV}_{\text{est}}) = 0.920 \log_{10}(P_d) + 1.642 \pm \sigma_{\text{PGV}_{\text{est}}} \qquad (2)$$

(PGV_{est} is in centimeters per second and P_d is in centimeters), where $\sigma_{\text{PGV}_{\text{est}}} = 0.326$.

For the real-time testing of the τ_c–P_d method within the SCSN, we have implemented the algorithm in an UNIX environment. We have chosen a modular design, so that modules can be easily changed, replaced, and/or added by new modules in order to improve the overall capabilities of the system. The processing steps are as follows: (1) retrieve velocity data from the SCSN (or the waveform storage); (2) set the baseline at zero by using average values continuously determined from the real-time data streams in intervals of 60 sec, and apply gain correction; (3) convert velocity to displacement by recursive integration; apply high-pass Butterworth filter (>0.075 Hz); (4) calculate τ_c and P_d from the initial 3 sec of waveform data.

To pick the seismic P phase we use a modification of an algorithm proposed by Allen (1978) in a combination with a simple P/S wave discriminator, which is based on the ratios of horizontal to vertical ground motions. To avoid false triggers, the system used station-dependent P_d thresholds for triggering. The thresholds ranged between 0.00004 and 0.0644 cm with an average of 0.0057 cm.

Data

For the time from 1 January 2007 to 31 December 2007, the SCSN reports 79 local earthquakes with $M_L \geq 3.0$ for southern California (see the Data and Resources section). P_d thresholds were exceeded for 40 of these events, triggering a total of 269 stations. During the same time period the system produced some thousand false triggers due to the generally low trigger thresholds set for initial testing.

Seven out of the nine earthquakes with $4.0 \leq M_L \leq 4.7$ (Fig. 1) were detected by the EEW algorithm; during events number 14330056 and 10285533, the EEW algorithm was not running. The number of reporting stations varied between 3 and 41 (Table 1). Averaged over the estimates from all reporting stations for all the seven events, the mean error of magnitudes M_{est}, estimated from period parameter τ_c in equation (1), is 0.5 units (Table 1). The magnitudes were usually slightly overestimated. The scatter of estimates is considerable, in particular for the smaller events with $M_L < 4.5$.

Table 1
Local Earthquakes in Southern California with $4.0 \leq M_L \leq 4.7$ in 2007 Used for EEW Testing

Event Identification Number	Date; Time (yyyy/mm/dd; hh:mm:ss UTC)	Latitude (°)	Longitude (°)	Depth (km)	M_L	Station-Dependent P_d Thresholds		New τ_c–P_d Trigger Criterion	
						Number of Reporting Stations	M_{est}	Number of Reporting Stations	M_{est}
10275733	2007/09/02; 17:29:14.790	33.7322	−117.4770	12.60	4.7	19	4.2 ± 0.8	44	4.3 ± 0.6
14312160	2007/08/09; 07:58:49.590	34.2995	−118.6195	7.58	4.6	19	4.8 ± 0.5	31	4.8 ± 0.4
14285168	2007/04/15; 22:57:26.720	32.6923	−116.0565	8.01	4.3	3	4.8 ± 0.5	5	5.0 ± 0.3
14330056	2007/10/24; 12:22:48.770	35.8380	−117.6847	4.50	4.3	—	—	9	4.5 ± 0.5
10230869	2007/02/09; 03:33:44.070	33.2113	−116.1480	12.00	4.2	41	4.4 ± 1.1	13	3.9 ± 0.5
10285533	2007/10/16; 08:53:44.120	34.3853	−117.6347	8.06	4.2	—	—	20	4.2 ± 0.4
14295640	2007/06/02; 05:11:26.470	33.8718	−116.2118	4.83	4.2	15	4.3 ± 1.4	11	3.9 ± 0.2
14282008	2007/03/30; 09:09:35.830	36.0277	−117.7753	0.35	4.0	10	5.4 ± 0.4	1	4.6
10295849	2007/12/19; 12:14:09.590	34.1555	−116.9820	10.22	4.0	16	4.6 ± 1.4	15	4.2 ± 0.4

For most events the number of reporting stations increases after application of the new τ_c–P_d trigger criterion (compared to the previously used station-dependent P_d thresholds) while the mean errors and standard deviations of estimated magnitudes M_{est} decrease (see the Data and Resources section).

Analyses of the corresponding distributions (Fig. 2) reveal that the standard deviations of M_{est} range from 0.5 to 1.4 magnitude units. Note that the scatter is mainly due to the records with poor S/N ratios, station drift, et cetera, rather than due to a failure of the τ_c-P_d algorithm itself. For the analyzed magnitude range $4.0 \leq M \leq 4.7$ we assume $M_L \approx M_w$ (Clinton *et al.*, 2006).

The τ_c-P_d Trigger Criterion

To improve the real-time performance of the τ_c-P_d algorithm, in particular for small- and moderate-sized events, we modified the previously used trigger algorithm based on station-dependent P_d thresholds with the aim (1) to decrease the number of false triggers, that is, triggers that cannot be
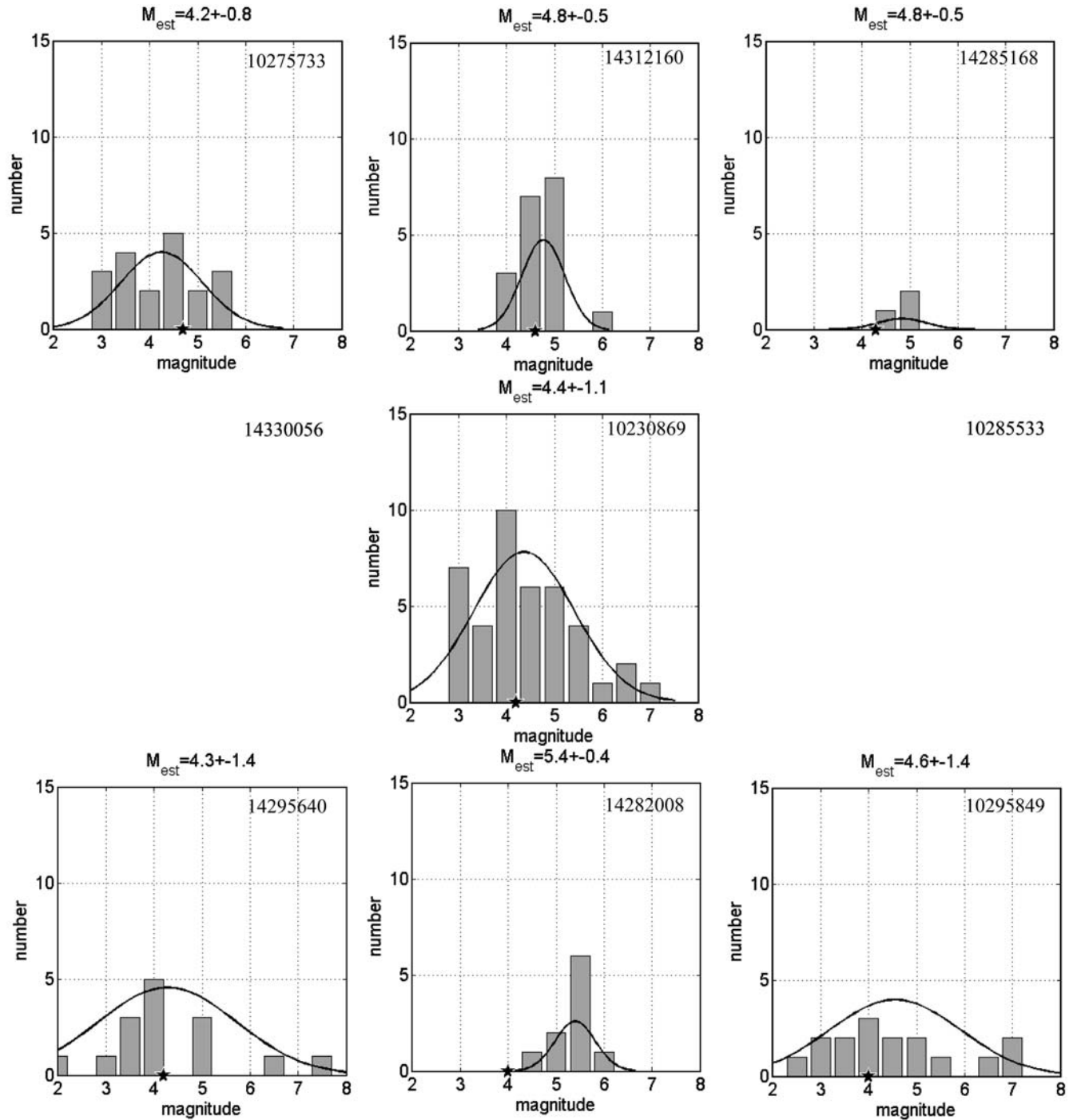

Figure 2.   Histograms for the estimated magnitudes M_{est} for the events in Table 1 obtained from the application of station-dependent P_d thresholds. Stars on the *x* axis show the magnitudes determined by SCSN. Note the high scatter in M_{est} in particular for earthquakes with $M_L \leq 4.5$. During two events, 14330056 and 10285533, the EEW algorithm was not running.

associated with any local earthquakes, (2) to reduce the scatter in M_{est}, that is, to automatically recognize earthquake records with poor S/N ratios, and (3) to increase the number of reporting stations with high S/N ratios that, however, did not pass the previously set P_d thresholds. The new trigger criterion is based on τ_c-dependent and therewith magnitude-dependent P_d thresholds. We call it τ_c–P_d trigger criterion.

The τ_c–P_d trigger criterion uses an empirical attenuation relation for PGV determined by G. Cua and T. Heaton (unpublished manuscript, 2008) based on earthquake records from southern California and the Next Generation Attenuation (NGA) strong-motion database. This relation is valid for earthquakes in the magnitude range $2.0 < M \leq 8.0$ and rupture-to-site distances $r \leq 200$ km. The relationship gives PGV as a function of r with the magnitude as a parameter. Using equations (1) and (2), we transform the function to a relation between P_d and r with τ_c as a parameter (see the Appendix), schematically shown in Figure 3 (left-hand panel). We then assume that only earthquakes within a certain distance range $r_{min} \leq r \leq r_{max}$ are relevant to EEW at a specific site. As shown in Figure 3 (left-hand panel), amplitude P_d has limiting values $P'_{d,max}$ and $P'_{d,min}$, corresponding to r_{min} and r_{max}, respectively. To illustrate the dependence of P_d on the period parameter, we plot in Figure 3 (right-hand panel) $P'_{d,min}$ (filled circles) and $P'_{d,max}$ (filled triangles) as a function of τ_c. If we consider the uncertainties in the τ_c–M_{est} relation (equation 1), the P_d–PGV_{est} relation (equation 2), and the empirical attenuation relation for PGV (G. Cua and T. Heaton, unpublished manuscript, 2008), we obtain P_d thresholds $P''_{d,min}$ and $P''_{d,max}$, as indicated by the two dashed curves in the right-hand panel of Figure 3 (see the Appendix for a more detailed explanation).

We formulate the τ_c–P_d trigger criterion as follows: for a given period parameter τ_c $(0.2 \leq \tau_c)$ and for a given displacement amplitude P_d $(P_d > P_{d,thres})$, both determined from the initial 3 sec of the P waveform data at a given station, we characterize the quality of the corresponding trigger by a parameter Q, which is defined by

right-hand panel). We judge the detected event to be associated with moderate data quality and assign $Q = 0.5$. In the third case (regions IIa or IIb in Fig. 3, right-hand panel), the trigger was likely caused by a distant earthquake $(r > r_{max})$, an earthquake with poor S/N ratio, or by noise. In this case we assign $Q = 0.0$. If $Q \geq 0.5$, M_{est} and PGV_{est} are computed. If $Q = 0.0$, the trigger is ignored.

Results

The τ_c–P_d diagram in Figure 4 shows the distribution of triggers produced by the onsite warning algorithm in southern California in 2007: correct triggers, associated with local earthquakes, are marked by dots and false triggers by x's. In order to extend the range of magnitudes, we also included 431 records of 27 Californian earthquakes with $4.2 \leq M \leq 7.3$ studied by Wu et al. (2007). We apply the τ_c–P_d trigger criterion with $r_{min} = 1$ km, $r_{max} = 100$ km, and $P_{d,thres} = 0.0005$ cm (which is about ten times smaller than the average value of the previously set station-dependent P_d thresholds) to these data.

As predicted, triggers caused by earthquakes tend to cluster between $P'_{d,min}$ and $P'_{d,max}$ (Fig. 4). Only a few of them lie between $P'_{d,min}$ and $P''_{d,min}$ or $P'_{d,max}$ and $P''_{d,max}$, respectively. False triggers, in contrast, tend to cluster outside these areas: they usually have high τ_c and low to moderate P_d values. Applying the new τ_c–P_d criterion to all triggers produced by the EEW algorithm in 2007, allows removing 97% of the former false triggers. Also, the number of earthquake triggers, which were earlier rejected due to the previously used station-dependent P_d thresholds, is increased. For instance, the number of reporting stations increases by 25 for the 2 September 2007 M_L 4.7 Elsinore earthquake, and by 12 for the 9 August 2007 M_L 4.6 Chatsworth earthquake (Table 1). For two events, 14330056 and 10285533, during which the EEW algorithm was not running, we obtain from archived data estimates from 9 and 20 reporting stations, respectively. For event 14282008 the observed ground

$$Q \equiv \begin{cases} 1.0, & \text{if } (P_d \geq P_{d,thres}) \quad \text{and} \quad (P_d \geq P'_{d,min}) \quad \text{and} \quad (P_d \leq P'_{d,max}), \\ 0.5, & \text{if } (P_d \geq P_{d,thres}) \quad \text{and} \quad \{[(P_d \geq P''_{d,min}) \quad \text{and} \quad (P_d \leq P'_{d,min})] \quad \text{or} \quad [(P_d \geq P'_{d,max}) \quad \text{and} \quad (P_d \leq P''_{d,max})]\}, \\ 0.0, & \text{else.} \end{cases}$$

$$(3)$$

In the first case, P_d is between $P'_{d,min}$ and $P'_{d,max}$ (region Ia in Fig. 3, right-hand panel) and the corresponding trigger was likely caused by a local earthquake within $r_{min} \leq r \leq r_{max}$. We judge the detected event is with good data quality and a high S/N ratio and assign $Q = 1.0$. In the second case, the value of the observed τ_c–P_d pair is between $P'_{d,min}$ and $P''_{d,min}$ or between $P'_{d,max}$ and $P''_{d,max}$ (region Ib in Fig. 3,

motion passes the new τ_c–P_d trigger criterion at only one close station.

Another positive effect is that the new τ_c–P_d trigger criterion significantly reduces the scatter of M_{est}. Figure 5 shows the recalculated levels of M_{est} for the earthquakes previously analyzed in Figure 2, which had been obtained from the station-dependent P_d thresholds. Averaged over the es-
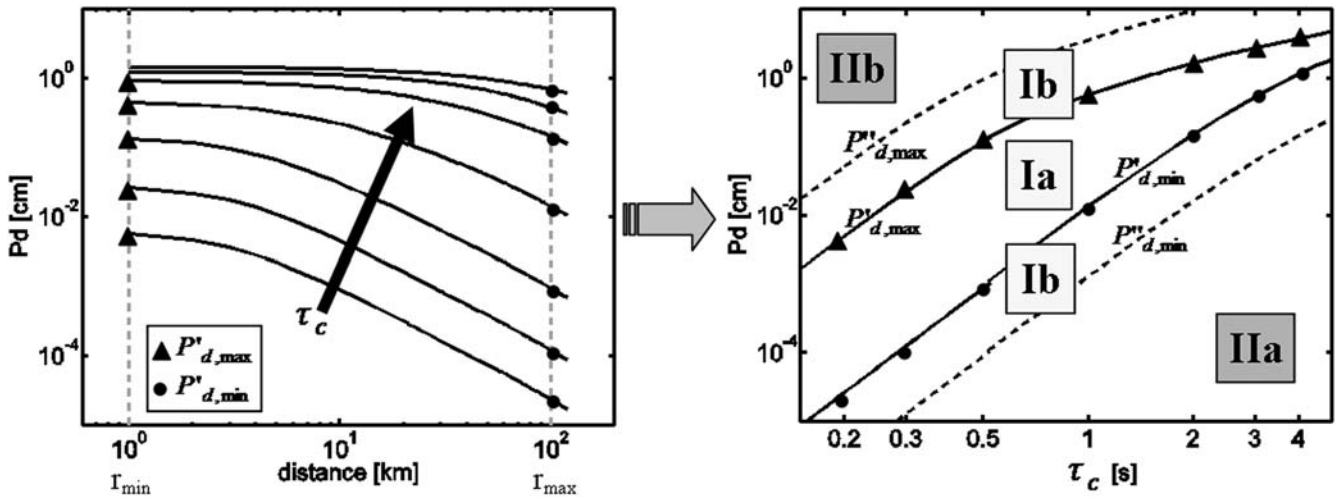
Figure 3. Illustration of the τ_c–P_d trigger criterion. Left-hand panel: Attenuation relations for P_d as a function of site-to-rupture distance r and period parameter τ_c; τ_c increases from bottom to top. The assumption that only earthquakes within a certain distance range $r_{min} \leq r \leq r_{max}$ are relevant to EEW at a specific site sets a constraint on the range of expected amplitudes P_d associated with r_{min}, $P'_{d,max}$, and r_{max}, $P'_{d,min}$. Right-hand panel: For continuous values of τ_c we obtain nonlinear discriminant functions (solid curves). Earthquakes with $r_{min} \leq r \leq r_{max}$ and high S/N ratios are expected to produce τ_c–P_d pairs within area Ia, while noisy data and distant earthquakes will generate τ_c–P_d combinations in region IIa. Spiky noise will be mapped onto region IIb. For EEW we shall only consider triggers that produce τ_c–P_d pairs within regions Ia and Ib. Region Ib accounts for the uncertainties of the underlying relations.

timates of all triggered stations for the nine events, the mean prediction error of M_{est} is 0.3 magnitude units. The standard deviations of estimates range between 0.2 and 0.6 magnitude units (Table 1).

Discussion and Conclusions

The τ_c–P_d onsite warning algorithm developed by Kanamori (2005) and Wu *et al.* (2007) has been implemented

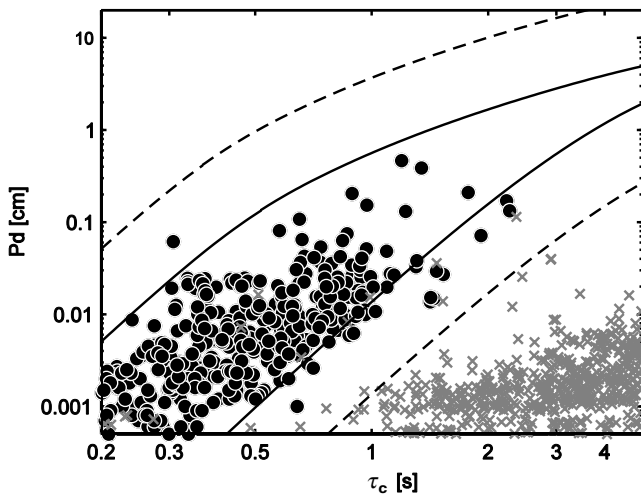**Figure 4.** τ_c–P_d diagram for earthquakes ($4.2 \leq M \leq 7.3$; Wu *et al.*, 2007) and false triggers in southern California. The majority of triggers produced by earthquakes (dots) can be clearly separated from false triggers (x's) by the discriminant functions of the τ_c–P_d trigger criterion (solid and dashed curves). For improved clarity we plot only false triggers produced during one month.

within the SCSN and tested for about 1 yr in a real-time environment. Although no large events that would require early warning occurred during 2007, the EEW algorithm processed seven local earthquakes with $4.0 \leq M_L \leq 4.7$. The high scatter in the estimated magnitudes for these small events can be significantly reduced after the application of a new τ_c–P_d trigger algorithm presented in this article. This criterion essentially removes all triggers that were likely caused by distant earthquakes, noise, or events with poor S/N ratios. At the same time the criterion allows reducing the number of false triggers by 97%, compared to the earlier used station-dependent P_d thresholds.

The earthquake 14282008 occurred 6 km east of Coso Junction, an area known for the frequent occurrence of earthquake swarms. The event was preceded by more than 20 foreshocks and followed by more than 30 aftershocks within a 5 min period (see the Data and Resources section). A small foreshock that occured 48 sec before the mainshock caused high-background noise level at the majority of close EEW stations before and during the arrival of the seismic P phase from the mainshock. Although such foreshocks are relatively rare, the real-time identification of such events will pose a major challenge in developing future EEW systems.

Mass-recentering of the sensors by the network operators can produce both large τ_c and P_d values within the areas Ia and Ib in Figure 3, right-hand panel, and, thus, can cause false triggers. We are developing capabilities in the EEW algorithm to automatically recognize these events by, for instance, evaluating the bias level of the signal. In the future, we plan joint analysis of waveforms from the colocated broadband and strong-motion instruments, which can be used for the elimination of calibration steps.
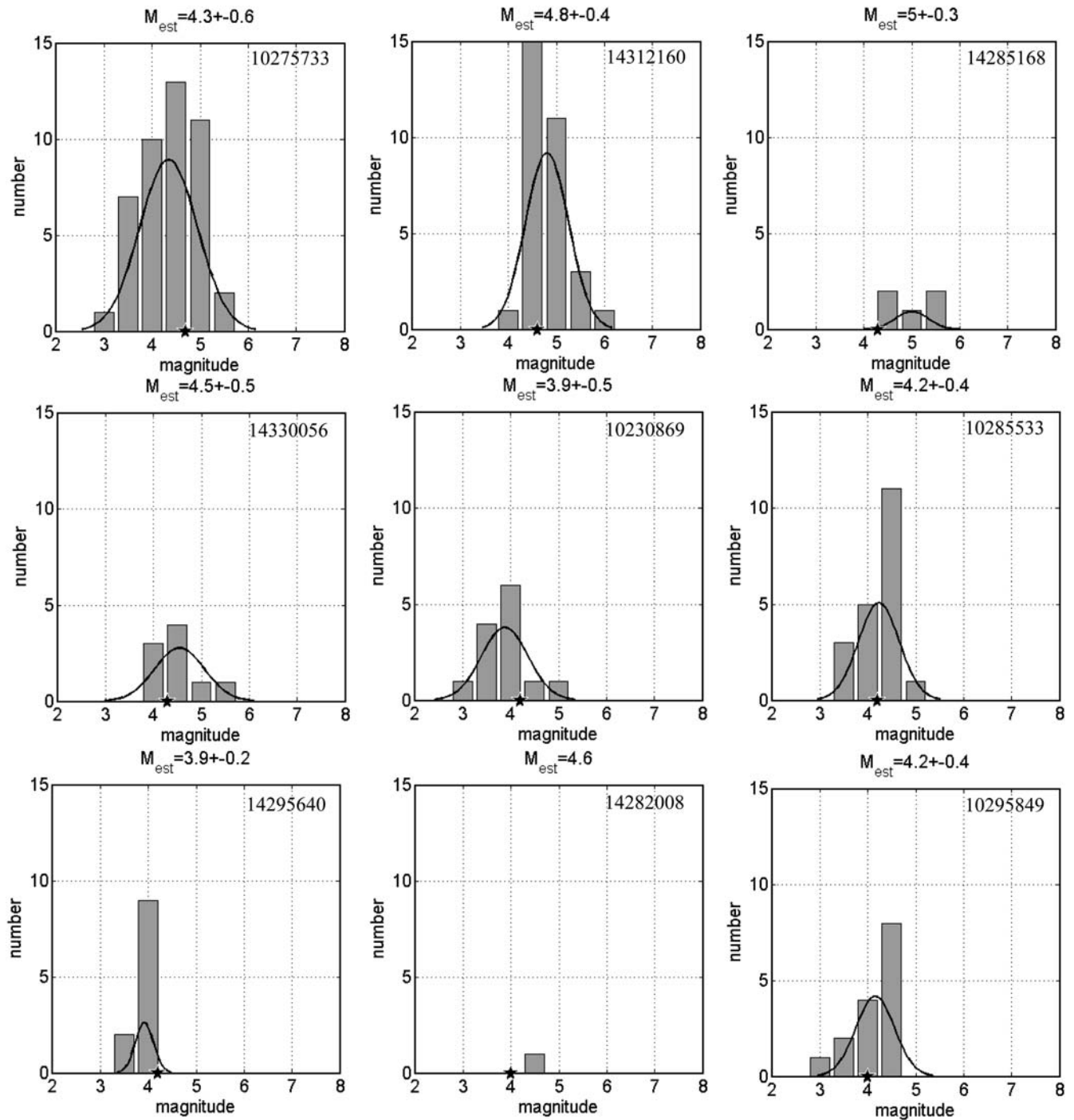
Figure 5. Histograms for the estimated magnitudes M_{est} for the events in Table 1 obtained after the application of the new τ_c–P_d trigger criterion. Stars on the x axis show the magnitudes determined by SCSN. The scatter of M_{est} is significantly reduced if compared with the estimates in Figure 2 because records with poor S/N are removed by the new criterion.

To consider the increasing areas of impacts by large earthquakes for which warnings are needed, one may possibly expect a dependency of r_{max} on magnitude and, thus, on τ_c. The current τ_c–P_d trigger criterion has been determined from an attenuation relation for PGV at rock sites. Thus, for stations built on soft soils, the impact of site effects might be significant. We tested if the usage of station-dependent magnitude corrections and V_{S30}-dependent PGV corrections, as used within the SCSN, can help to reduce the scattering of the data in Figure 4. However, because P and S waves are affected differently by site conditions, site corrections for τ_c magnitude and P_d–PGV relations in equations (1) and (2) are complex, and common P or S correction factors cannot be applied. Unfortunately, because of a lack of data, the current database does not allow for a reliable analysis of correction terms separately for each SCSN station.

The current early warning system tested in southern California uses a time window of $\tau_0 = 3$ sec length to determine the early warning parameters τ_c and P_d. As pointed out by Rydelek and Horiuchi (2006) or Rydelek *et al.* (2007), this time window might possibly be too short for the determination of magnitudes larger than 6.5, because of the long rupture durations of large earthquakes. The available data indicate that it is possible to recognize from this 3 sec time window if $M_w \leq 6.5$ or $M_w > 6.5$ (Kanamori, 2005). We chose the 3 sec length as a compromise between knowing it is a large magnitude earthquake and not waiting too long to evaluate the available data. Additional research needs to be undertaken to verify if a 3 sec long window is optimal, which may include the approach of threshold warning as recently proposed in Wu and Kanamori (2008b). However, the trigger criterion used in this study is not affected by the duration of the time window used.

Of course, small- and moderate-sized earthquakes with $M < 6.0$ as analyzed in this study will usually not cause damage to buildings, equipment, or humans. For the automatic recognition of large earthquakes Wu and Kanamori (2005a,b, 2008a,b) and Wu *et al.* (2006, 2007) propose to test whether the criterion $\tau_c > 1$ sec and $P_d > 0.5$ cm is fulfilled. These large events will likely not be affected by the problem of poor S/N ratios addressed in this study. However, it is necessary to use the more frequent small events for testing and calibration of EEW algorithms because large earthquakes are rare. Thus, the lessons learned from this study of small earthquakes will form the basis for future enhancements of EEW algorithms and understanding of their robustness in real-time applications.

Data and Resources

Waveform data used in this study (Table 1) are taken from the Southern California Earthquake Data Center (www.data.scec.org, last accessed March 2008). Figure 1 was made using the Generic Mapping Tools version 4.2.1 (Wessel and Smith, 1998; www.soest.hawaii.edu/gmt, last accessed March 2008).

Acknowledgments

References

Allen, R. M. (2007). The ElarmS earthquake early warning methodology and its application across California, in *Earthquake Early Warning Systems*, P. Gasparini, G. Manfredi and J. Zschau (Editors), 21–44, Springer, Berlin Heidelberg.

Allen, R. M., and H. Kanamori (2003). The potential for earthquake early warning in southern California, *Science* **300,** 786–789.

Allen, R. V. (1978). Automatic earthquake recognition and timing from single traces, *Bull. Seismol. Soc. Am.* **68,** 1521–1532.

Böse, M., C. Ionescu, and F. Wenzel (2007). Earthquake early warning for Bucharest, Romania: novel and revised scaling relations, *Geophys. Res. Lett.* **34,** L07302, doi 10.1029/2007GL029396.

Böse, M., F. Wenzel, and M. Erdik (2008). PreSEIS: a neural network based approach to earthquake early warning for finite faults, *Bull. Seismol. Soc. Am.* **98,** no. 1, 366–382, doi 10.1785/0120070002.

Clinton, J. F., E. Hauksson, and K. Solanki (2006). An evaluation of the SCSN moment tensor solutions: robustness of the M_w magnitude scale, style of faulting, and automation of the method, *Bull. Seismol. Soc. Am.* **96,** no. 5 1689–1705, doi 10.1785/0120050241.

Cua, G., and T. Heaton (2007). The virtual seismologist (VS) method: a Bayesian approach to earthquake early warning, in *Earthquake Early Warning Systems*, P. Gasparini, G. Manfredi and J. Zschau (Editors), 85–132, Springer, Berlin Heidelberg.

Erdik, M., Y. Fahjan, O. Ozel, H. Alcik, A. Mert, and M. Gul (2003). Istanbul earthquake rapid response and the early warning system, *Bull. Earthq. Eng.* **1,** 157–163.

Espinosa-Aranda, J., A. Jiménez, G. Ibarrola, F. Alcantar, A. Aguilar, M. Inostroza, and S. Maldonado (1995). Mexico City seismic alert system, *Seism. Res. Lett.* **66,** 42–53.

Goltz, J. (2002). Introducing earthquake early warning in California: a summary of social science and public policy issues, a report to OES and the Operational Areas, Caltech Seismological Laboratory, Disaster Assistance Division.

Harben, P. (1991). Technical Report UCRL-LR-109625: Earthquake alert system feasibility study, Lawrence Livermore National Laboratory, Livermore, California.

Hauksson, E., P. Small, K. Hafner, R. Busby, R. Clayton, J. Goltz, T. Heaton, K. Hutton, H. Kanamori, J. Polet, D. Given, L. M. Jones, and D. Wald (2001). Southern California Seismic Network: Caltech/USGS element of TriNet 1997–2001, *Seism. Res. Lett.* **72,** 690–704.

Hauksson, E., K. Solanki, D. Given, P. Maechling, D. Oppenheimer, D. Neuhauser, and P. Hellweg (2006). Implementation of real-time testing of earthquake early warning algorithms: using the California Integrated Seismic Network (CISN) infrastructure as a test bed (abstract), *Seismol. Soc. Am. Annual Meeting*, San Francisco, California, 18–22 April 2006.

Horiuchi, S., H. Negishi, K. Abe, A. Kamimura, and Y. Fujinawa (2005). An automatic processing system for broadcasting earthquake alarms, *Bull. Seismol. Soc. Am.* **95,** 708–718.

Kamigaichi, O. (2004). JMA earthquake early warning, *J. Jpn. Assoc. Earthq. Eng.* **4,** 134–137.

Kanamori, H. (2005). Real-time seismology and earthquake damage mitigation, *Annu. Rev. Earth Planet. Sci.* **33,** 195–214, doi 10.1146/annurev.earth.33.092203.122626.

Nakamura, Y. (1988). On the urgent earthquake detection and alarm system (UrEDAS), *Proceeding of the 9th World Conference on Earthquake Engineering*, Tokyo-Kyoto, Japan.

Rydelek, P., and S. Horiuchi (2006). *Is the earthquake rupture deterministic? Nature* **442,** E5–E6, doi 10.1038/nature04963.

Rydelek, P., C. Wu, and S. Horiuchi (2007). Comment: peak ground displacement and earthquake magnitude, *Geophys. Res. Lett.* **34,** L20302, doi 10.1029/2007GL029387.

Tsukada, S., O. Kamigaichi, M. Saito, K. Takeda, T. Shimoyama, K. Nakamura, M. Kiyomoto, and Y. Watanabe (2007). Provision of earthquake early warning to the general public and necessary preparatory process in Japan, (Abstract S21D-01), *EOS Trans. AGU*, **88,** no. 52 (Fall Meet. Suppl.), S21D-01.

Wenzel, F., M. Oncescu, M. Baur, and F. Fiedrich (1999). An early warning system for Bucharest, *Seism. Res. Lett.* **70,** no. 2, 161–169.

Wessel, P., and W. H. F. Smith (1998). New, improved version of the Generic Mapping Tools Released, *EOS Trans. AGU* **79,** 579.

Wu, Y. M., and H. Kanamori (2005a). Experiment on an onsite early warning method for the Taiwan early warning system, *Bull. Seismol. Soc. Am.* **95,** 347–353.

Wu, Y. M., and H. Kanamori (2005b). Rapid assessment of damaging potential of earthquakes in Taiwan from the beginning of *P* waves, *Bull. Seismol. Soc. Am.* **95,** 1181–1185.

Wu, Y. M., and H. Kanamori (2008a). Development of an earthquake early warning system using real-time strong motion signals, *Sensors* **8,** 1–9.

Wu, Y. M., and H. Kanamori (2008b). Exploring the feasibility of on-site earthquake early warning using close-in records of the 2007 Noto Hanto earthquake, *Earth Planets Space* **60,** 155–160.

Wu, Y. M., and T. L. Teng (2002). A virtual sub-network approach to earthquake early warning, *Bull. Seismol. Soc. Am.* **92,** 2008–2018.

Wu, Y.-M., H. Kanamori, R. M. Allen, and E. Hauksson (2007). Determination of earthquake early warning parameters, τ_c and P_d, for southern California, *Geophys. J. Int.* **170,** 711–717, doi 10.1111/j.1365-246X.2007.03430.x.

Wu, Y. M., H. Y. Yen, L. Zhao, B. S. Huang, and W. T. Liang (2006). Magnitude determination using initial *P* waves: a single-station approach, *Geophys. Res. Lett.* **33,** L05306, doi 10.1029/2005GL025395.

Wurman, G., R. M. Allen, and P. Lombard (2007). Toward earthquake early warning in northern California, *J. Geophys. Res.* **112,** B08311, doi 10.1029/2006JB004830.

Appendix

Mathematical Description of the Trigger Criterion

The reformulation of the empirical attenuation relation for PGV established by G. Cua and T. Heaton (unpublished manuscript, 2008) in terms of displacement amplitude P_d gives

$$P'_{d,\min}$$

$$= 10^{[(\log_{10}\{10^{aM_{\mathrm{est}}+b[R_{\max}+C(M_{\mathrm{est}})']}+d\log_{10}[R_{\max}+C(M_{\mathrm{est}})']+e\}f\}-1.642)/0.92]}$$

(A1)

and

$$P'_{d,\max}$$

$$= 10^{[(\log_{10}\{10^{aM_{\mathrm{est}}+b[R_{\min}+C(M_{\mathrm{est}})']}+d\log_{10}[R_{\min}+C(M_{\mathrm{est}})']+e\}f\}-1.642)/0.92]},$$

(A2)

with $a = 0.86$, $b = -0.000558$, $d = -1.37$, $e = -2.58$, $R_{\min} = \sqrt{r_{\min}^2 + 9}$, $R_{\max} = \sqrt{r_{\max}^2 + 9}$, and $C(M_{\mathrm{est}})' = c_1 \exp[c_2(M_{\mathrm{est}} - 5)][\arctan(M_{\mathrm{est}} - 5) + \pi/2]$, with $c_1 = 0.84$ and $c_2 = 0.98$. The parameter f in equations (A1) and (A2) makes the conversion from root mean square horizontal PGV to maximum horizontal PGV. Following G. Cua (personal communication, 2008), we set $f = 1.1$.

Accounting for the uncertainties of all relations involved in equations (A1) and (A2) we obtain, in addition

with

$$C(M_{\mathrm{est}})'' = c_1 \exp[c_2(M_{\mathrm{est}} - \sigma_{M_{\mathrm{est}}} - 5)]$$
$$\times [\arctan(M_{\mathrm{est}} - \sigma_{M_{\mathrm{est}}} - 5) + \pi/2],$$

and

$$C(M_{\mathrm{est}})''' = c_1 \exp[c_2(M_{\mathrm{est}} + \sigma_{M_{\mathrm{est}}} - 5)]$$
$$\times [\arctan(M_{\mathrm{est}} + \sigma_{M_{\mathrm{est}}} - 5) + \pi/2],$$

respectively. The standard deviations $\sigma_{M_{\mathrm{est}}}$ and $\sigma_{\mathrm{PGV_{est}}}$ are determined in equations (1) and (2), and $\sigma_{IM} = 0.28$ (for rock sites; G. Cua and T. Heaton, unpublished manuscript, 2008).

Seismological Laboratory
California Institute of Technology
1200 E. California Boulevard
Mail Code 252-21
Pasadena, California 91125
mboese@gps.caltech.edu
hauksson@gps.caltech.edu
solanki@gps.caltech.edu
hiroo@gps.caltech.edu
heaton@gps.caltech.edu
    (M.B., E.H., K.S., H.K., T.H.H.)

Department of Geosciences
National Taiwan University
Taipei, Taiwan
drymwu@ntu.edu.tw
    (Y.-M.W.)

$$P''_{d,\min} = 10^{[(\log_{10}\{10^{a(M_{\mathrm{est}}-\sigma_{M_{\mathrm{est}}})+b[R_{\max}+C(M_{\mathrm{est}})'']}+d\log_{10}[R_{\max}+C(M_{\mathrm{est}})'']+e-\sigma_{IM}\}f\}-1.642-\sigma_{\mathrm{PGV}})/0.92]},$$

(A3)

and

$$P''_{d,\max} = 10^{[(\log_{10}\{10^{a(M_{\mathrm{est}}+\sigma_{M_{\mathrm{est}}})+b[R_{\min}+C(M_{\mathrm{est}})''']}+d\log_{10}[R_{\min}+C(M_{\mathrm{est}})''']+e+\sigma_{IM}\}f\}-1.642+\sigma_{\mathrm{PGV}})/0.92]},$$

(A4)